DYNAMIC RUNNING QUADRUPED FOR CRATER EXPLORATION

Ioannis Kontolatis, Evangelos Papadopoulos
Control Systems Laboratory, Department of Mechanical Engineering,
National Technical University of Athens,
9, Heroon Polytexneiou Str., 15780 Zografou, Athens, Greece
Email: ikontol@central.ntua.gr, egpapado@central.ntua.gr

ABSTRACT

This paper presents simulation results obtained with a planar lumped parameter model of a quadruped robot during a crater exploration mission in Earth, Mars and Moon-like gravity environments. First, simulations were conducted to validate ideal values of VLegs spring constant when the quadruped robot traverses a level terrain. Next, simulations were conducted to validate the maximum values of negative and positive slope according to forward speed in the three gravity environments. Experiments with the NTUA Quadruped, were conducted to validate the simulation environment. Experimental results obtained using internal sensors show that the quadruped robot performs gaits with the desired characteristics and in accordance to simulations.

1. INTRODUCTION

Celestial body surface exploration using robotic systems aims for answering crucial scientific questions, e.g. geologic evolution, evidence of extinct or extant life, or gathering valuable information for future manned missions, e.g. potential landing sites. These environments are highly unstructured and their terrain morphology changes over few meters.

Areas of increased scientific interest and therefore targets for exploration are hydrothermal vents, craters, ditches, basins and volcanoes [1]. One realistic mission scenario for a robotic surface explorer is to travel from the landing site to the edge of an impact crater (Fig. 1), descend to its floor, collect samples or conduct an experiment, and finally ascend and return to base.

Figure 1. Impact crater structure. NASA, 2003.

Rovers have proved to be a successful solution. Spirit and Opportunity have exceeded even the wildest expectations of scientists and engineers. Although rovers succeed in traversing almost level terrains with obstacles of certain size, their performance is low in sloped terrains and thus areas of great scientific importance are beyond their safe reach.

An alternative to the wheeled robotic explorers is a mobile platform using a legged locomotion system, like the one in Fig. 2. Engineers have already acknowledged the potential advantages of such systems and presented concept designs and addressed possible issues.

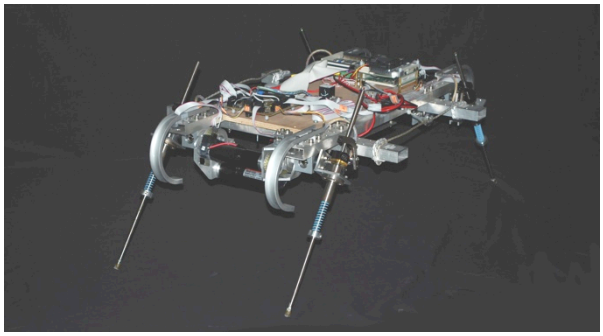

Figure 2. The NTUA Quadruped robot.

To name a few, researchers at the JPL proposed the ATHLETE concept, a six-limbed hybrid mobile platform designed to traverse terrain using its wheels or limbs [2]. The robots of the ATHLETE family have increased mechanical complexity and use statically stable gaits, without capability of quick motions or right themselves from an unstable position. Another six-legged robot proposed for planetary exploration is the DLR Crawler [3], an actively compliant walking robot that implements a walking layer with a simple tripod and a more complex biologically inspired gait. Nevertheless, the robot lacks a planner for footholds and body poses to handle highly uneven terrains. The robot ASTRO, part of an emulation testbed for asteroid exploration, is a six-limbed ambulatory locomotion system that replicates walking gaits of the arachnid insects to avoid surface ejection [4]. DFKI researchers presented SpaceClimber, a biologically inspired six-legged robot for steep slopes, and focused on the foot-design of the robot to handle constraints from the environmental ground conditions [5]. The robot exploits a Central Pattern Generator (CPG) and although it handles slopes around 25^{o}, its forward speed is quite slow, i.e. 125 mm/s, which is expected for a statically stable gait. Researchers from ASL/ ETH proposed a quadruped concept design for planetary exploration that was built for upright walking but its wide range of motion in all joints allows a crawling gait when loose soil or steep slopes are encountered and recovery manoeuvres after tipping over [6].

These robots perform statically stable gaits for the sake of overall motion stability and rough terrain handling, which reduces their speed capability. On the other hand, mission time is valuable and a reduction in travel time between targets of interest would be to the benefit of time conducting scientific experiments. A legged robot that exploits dynamically stable gaits can achieve higher speeds, but it is subjected to complex motion control challenges and balance-in-motion constraints, especially when handling sloped terrains.

In this paper, we use a lumped parameter planar model of a quadruped robot and conduct simulation experiments to verify the effect of leg stiffness and length to motion characteristics and energy requirements. In addition, we run simulations of a crater exploration mission scenario. Travel speed, overall motion stability and energy efficiency criteria are taken into consideration. Also, we vary gravity to emulate the Mars or the Moon environment. We assume that ground forces exerted on leg toe are always in the friction cone and that there is absence of leg sinkage. In addition, we use the NTUA Quadruped (Fig. 2) to conduct experiments in Earth's gravity and evaluate the effect of leg stiffness upon motion parameters, i.e. forward speed and pitch. The results will be used to validate the simulation environment for different gravity conditions.

2. QUADRUPED ROBOT DYNAMICS

2.1. Robot Model

A lumped parameter model of a quadruped robot depicted in Fig.3 used in simulations. The model consists of two compliant virtual legs (VLegs) of mass m_j and inertia I_j and a body of m, I respectively. The index j indicates rear (r) or front (f) VLeg. A VLeg, front or rear, models the two respective physical legs that operate in pairs when a gait is realized and exerts equal torques and forces on the body as the set of the physical ones [7].

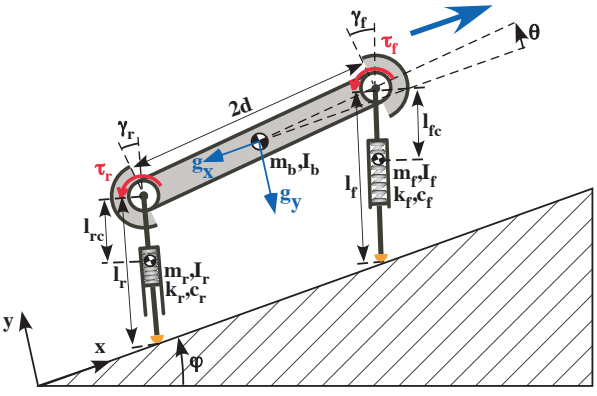

Figure 3. A lumped parameter planar quadruped model.

Each VLeg is connected to the body with an actuated rotational joint at distance d from body center of mass (CM). The body can rotate at an angle θ around z-axis of its CM and thus the model captures the body pitch stabilization problem. The rotational hip joint allows positioning of VLegs at angle γ_j in the sagittal plane. Also, each VLeg has a passive prismatic joint modeled as a linear compression spring of constant k_j and viscous dumping coefficient c_j. It should be noted that front and rear VLegs are modeled in general to have different uncompressed length l_{0j}, spring constant k_j and viscous damping coefficient c_j. The prismatic joint allows changes of the VLeg length l_j and energy accumulation during locomotion. Table 1 summarizes model and motion parameters. The planar model is valid for gaits that have symmetry about the plane of the forward motion, like pronking and bounding; these will be realized during simulations and experiments.

Table 1. Nomenclature.

Symbol	Quantity
x_c	Body CM x-axis coordinate
y_c	Body CM y-axis coordinate
θ	Body pitch angle
I_b	Body inertia w.r.t. z-axis
m_b	Body mass
x	VLeg CM x-axis coordinate
y	VLeg CM y-axis coordinate
l	VLeg length
l_0	VLeg uncompressed length
k	VLeg spring constant
c	VLeg viscous dumping coefficient
γ	VLeg absolute angle
I_l	VLeg inertia w.r.t. z-axis
m	VLeg mass
d	Hip joint to CM distance
φ	Ground inclination
τ	Hip torque
r	As index: rear VLeg
f	As index: front VLeg
td	As index: value at touchdown
lo	As index: value at liftoff

2.2. Motion Phases and Transitions

A quadruped robot, studied in the sagittal plane, has four potential configurations of the three-link (rear VLeg, front VLeg, main body) kinematic chain, i.e. double stance, flight, front stance, rear stance, as presented in Fig. 4. The realization of the gait depends on which legs are working in pairs, which motion phases appear and for how long, the values of the leg touchdown angles and body pitch angle.

Pronking is the type of gait when all legs are in the same phase, either in contact with ground (double stance) or not (flight). The bounding gait has two additional intermediate phases, namely the ones when only one set of legs (rear or front) is in contact with the ground. In pronking, zero or close to zero pitching is

expected. However, in the non-ideal case, where body pitching occurs, the rear or front legs may strike the ground first. Then, pronking reduces to a bounding gait.

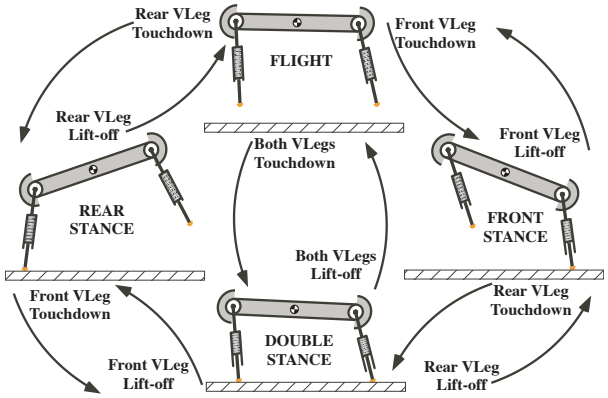

Figure 4. Motion Phases and Events that trigger them.

Legged robots are hybrid systems and therefore their motion cannot be described by a single set of equations. A collection of continuous equations for each phase together with discrete transformations governing transitions from one phase to the next are required to model the dynamics of such systems. The transition equations that determine the touchdown and lift-off events of the rear and front VLegs during sagittal plane motion are given by the following equations:

$$y_c - dSin(\theta_{td}) \le l_{0r} Cos(\gamma_{r,td}) \quad (1)$$

$$y_c + dSin(\theta_{td}) \le l_{0f} Cos(\gamma_{f,td}) \quad (2)$$

$$l_{r,lo} = l_{0r} \quad (3)$$

$$l_{f,lo} = l_{0f} \quad (4)$$

The Eq. (1) and (2) describe the conditions of rear and front VLeg touchdown events respectively, while Eq. (3) and (4) describe the conditions of rear and front VLeg liftoff events. All conditions are based in length comparison. In Tab. 2 is summarized which event trigger equations are checked in each phase.

Table 2. Event trigger equation for each motion phase.

Motion Phase	Event Equations
Flight	Eq. (1), Eq. (2)
Rear Stance	Eq. (2), Eq. (3)
Double Stance	Eq. (3), Eq. (4)
Front Stance	Eq. (1), Eq. (4)

Equations of Motion

The robot motion is studied in the sagittal plane. During the flight phase (both VLegs do not touch the ground), the robot's CM performs a ballistic motion with constant system angular momentum with respect to the CM. During stance phase the VLeg(s) that are in contact with the ground move the body forward.

The equations of motion for the main phases, i.e. flight and double stance, and for the intermediate ones, i.e. front and rear stance, are derived using the Lagrange formulation with the vector

$$\mathbf{q} = \begin{bmatrix} x_c & y_c & \theta & l_r & \gamma_r & l_f & \gamma_f \end{bmatrix} \quad (5)$$

as the set of the generalized coordinates. The Lagrangian of the rear and front VLeg and the body are:

$$L_{VLegr} = \frac{1}{2} m_r (\dot{x}_r^2 + \dot{y}_r^2) - \frac{1}{2} k_r (l_{0r} - l_r)^2 - m_r g_x x_r - m_r g_y y_r \quad (6)$$

$$L_{VLegf} = \frac{1}{2} m_f (\dot{x}_f^2 + \dot{y}_f^2) - \frac{1}{2} k_f (l_{0f} - l_f)^2 - m_f g_x x_f - m_f g_y y_f \quad (7)$$

$$L_{Body} = \frac{1}{2} m_b (\dot{x}_c^2 + \dot{y}_c^2) + \frac{1}{2} I_b \dot{\theta}^2 - m_b g_x x_c - m_b g_y y_c \quad (8)$$

while the Lagrangian of the robot is given by summing Eq. (6) – (8):

$$L_{Robot} = L_{Body} + L_{VLegr} + L_{VLegf} \quad (9)$$

Rear (x_r, y_r) and front (x_f, y_f) VLeg CM coordinates can be expressed as functions of the generalized coordinates using geometrical relationships:

$$x_r = x_c - dCos(\theta) + l_{rc} Sin(\gamma_r)$$
$$y_r = y_c - dSin(\theta) - l_{rc} Cos(\gamma_r) \quad (10)$$

$$x_f = x_c + dCos(\theta) + l_{fc} Sin(\gamma_f)$$
$$y_f = y_c + dSin(\theta) - l_{fc} Cos(\gamma_f) \quad (11)$$

The energy dissipation due to prismatic joint viscous damping is:

$$P_{Diss} = \frac{1}{2} c_r \dot{l}_r^2 + \frac{1}{2} c_f \dot{l}_f^2 \quad (12)$$

The energy contribution of actuator torques is given by:

$$P_{Contr} = \tau_r (\dot{\gamma}_r - \dot{\theta}) + \tau_f (\dot{\gamma}_f - \dot{\theta}) \quad (13)$$

Equations of motion for all phases derive from [8]:

$$\frac{d}{dt}\left(\frac{\partial L_{Robot}}{\partial \dot{\mathbf{q}}}\right)^T - \left(\frac{\partial L_{Robot}}{\partial \mathbf{q}}\right)^T + \left(\frac{\partial P_{Diss}}{\partial \dot{\mathbf{q}}}\right)^T - \left(\frac{\partial P_{Contr}}{\partial \dot{\mathbf{q}}}\right)^T = \mathbf{0} \quad (14)$$

For the double stance phase, vector **q** includes only variables x_c, y_c and θ, while the rest derive using geometrical relationships:

$$l_r = \sqrt{(x_{r,td} + dCos(\theta) - \chi_c)^2 + (dSin(\theta) - y_c)^2} \quad (15)$$

$$\gamma_r = A\tan(-dSin(\theta) + y_c, x_{r,td} + dCos(\theta) - \chi_c) \quad (16)$$

$$l_f = \sqrt{(x_{f,td} - dCos(\theta) - \chi_c)^2 + (dSin(\theta) - y_c)^2} \quad (17)$$

$$\gamma_f = A\tan(dSin(\theta) + y_c, x_{f,td} - dCos(\theta) - \chi_c) \quad (18)$$

The quantities $x_{r,td}$ and $x_{f,td}$ are given by:

$$x_{r,td} = x_c + l_r Sin(\gamma_r) - dCos(\theta) \quad (19)$$

$$x_{f,td} = x_c + l_f Sin(\gamma_f) + dCos(\theta) \quad (20)$$

when touchdown occurs. At this point, we note that no toe slippage is assumed.

For the two intermediate phases, i.e. rear and front stance, vector **q** does not include l_r, γ_r and l_f, γ_f respectively, which are calculated again by Eq. (15), (16) and Eq. (17), (18). Also, the ground inclination, positive or negative, affects robot dynamics through the two gravity components g_x, g_y:

$$g_x = g \cdot Sin(\varphi), \qquad g_y = g \cdot Cos(\varphi) \quad (21)$$

3. SIMULATIONS

The quadruped robot model presented in section 2 used in simulations. The multipart controller presented in [9], based on the energy transfer mechanism ETM, assures that the robot motion will have specific characteristics, i.e. forward speed and apex height, and will be maintained constant around desired values.

The robot is released with its CM 0.35 m above the ground with zero pitch angle and 0.5 rad / s pitch angle rate, while it has zero vertical velocity and forward speed of 0.4 m /s. The motion of the robot body is constrained to the sagittal plane. The simulation stops when the robot has completed 100 gaits, i.e. complete cycles considered from one flight phase until the next. While the desired forward speed varies, the desired apex height of robot CM is constant, 0.32 m above the ground.

3.1. Level Terrain

Simulations were conducted to validate ideal values of VLegs spring constant when the quadruped robot traverses a level terrain in three different gravity environments that emulate Moon, Mars and Earth. The results presented in Fig. 5 show that a region for every environment can be identified that provides self-stabilizing characteristics and makes achievable different values of forward speed. It is obvious, and expected, that as gravity drops the VLeg springs need to be softer to accumulate energy efficiently. Also, the maximum achievable forward speed is lower in Mars and even lower in the Moon. In addition, as leg springs become stiffer, torque requirements increase.

In Fig. 6 an example for zero and 10 degrees slope in earth gravity is presented. The use of softer springs leads to larger variations of robot body pitch angle. Fig. 7 shows the robot pitch angle variation with VLegs of 2200 and 6000 N/m in earth gravity simulations.

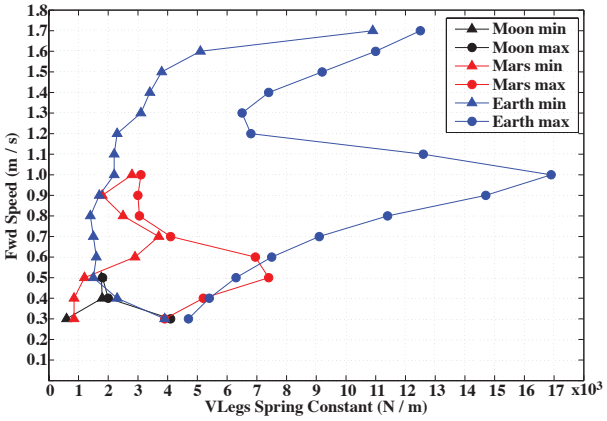

Figure 5. Spring constant values and corresponding fwd speed for different gravity. Level terrain.

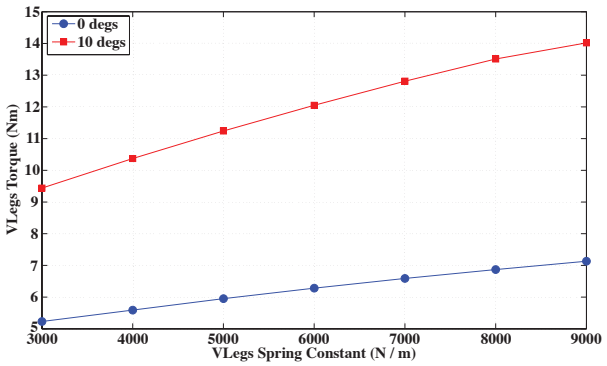

Figure 6. Actuator torque requirements for different VLegs spring constant. Level and sloped terrain.

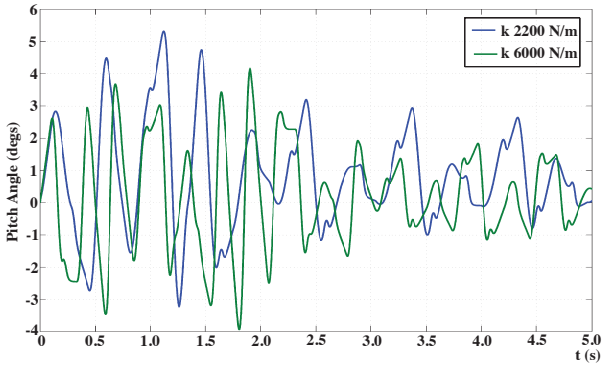

Figure 7. Pitch angles for VLeg spring constants.

3.2. Sloped Terrain

Simulations were conducted to validate the maximum values of negative and positive slope according to forward speed in the three gravity environments. The results are presented in Fig. 8. In all the three cases, the quadruped can handle steeper slopes when reduces its speed. Also, in most cases, it is necessary the VLeg stiffness to be altered. It should be noted here that the maximum VLeg torque requirements for this performance do not exceed specific value, i.e. 14Nm. This value corresponds to the limitations of the real DC

motors, like the ones the NTUA Quadruped uses.

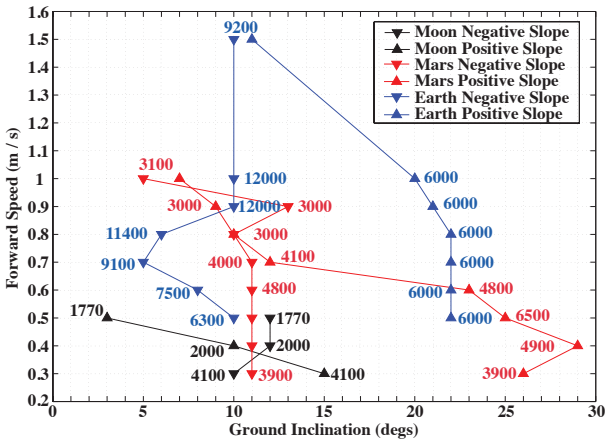

Figure 8. Achievable forward speed corresponding to ground inclination.

3.3. Crater Mission

Simulation were conducted based on the results of sections 3.1 and 3.2 and a crater exploration mission scenario. This mission scenario, as depicted in Fig. 9, involves traversing level terrain until the edge of the crater, descending a steep slope, traversing the almost level terrain of the crater floor, ascending a steep slope and again traversing a level terrain.

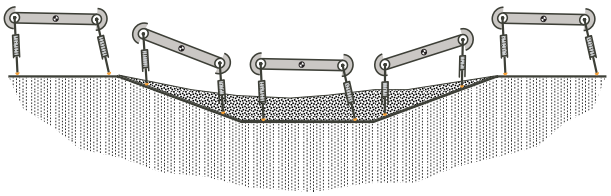

Figure 9. Quadruped motion during crater exploration.

In the case of a Mars-like gravity environment, the quadruped robot achieves and maintains a forward speed between 0.8 and 0.9 m/s (Fig. 10) during the mission, while the body pitch angle maximum values are ±4 degrees during transient phase (Fig. 11).

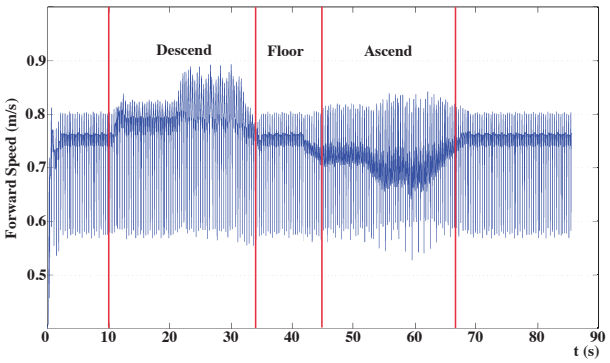

Figure 10. Forward speed during Mars crater exploration scenario.

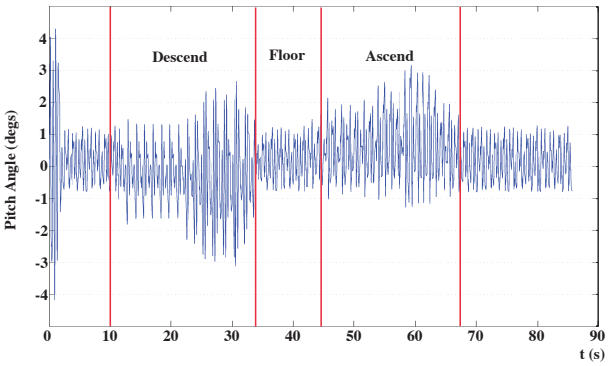

Figure 11. Body pitch angle during Mars crater exploration scenario.

In the case of a Moon-like gravity environment, the quadruped robot achieves and maintains a forward speed between 0.4 and 0.5 m/s (Fig. 12) during the mission, while the body pitch angle maximum values are ±5.7 degrees during transient phase (Fig. 13).

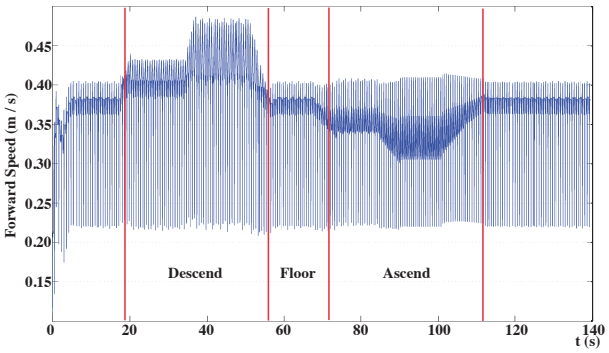

Figure 12. Forward speed during Moon crater exploration scenario.

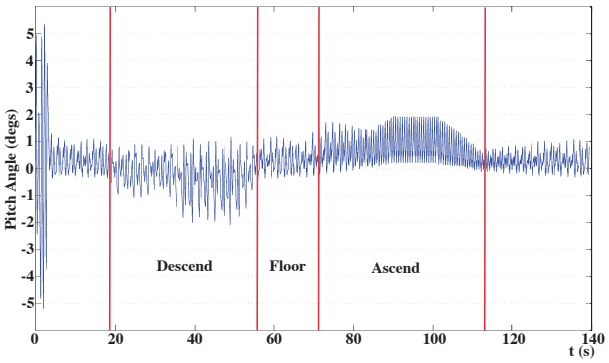

Figure 13. Body pitch angle during Moon crater exploration scenario.

4. NTUA QUADRUPED EXPERIMENTS

4.1. Hardware Description

The NTUA Quadruped (Fig.2) has legs with springs and only one actuator per each hip joint. The total mass of the robot is 11 kg, including motors, gearboxes, sensors,

electronics, LiPo batteries and onboard computer. All robot design parameters have been selected following a systematic methodology and are optimal according to selected performance criteria [10]. These criteria are (a) minimization of energy requirements to sustain a certain motion and (b) maximization of payload capability for the target robot mass. Tab. 3 summarizes the NTUA Quadruped physical parameters.

Table 3. NTUA Quadruped physical parameters.

Parameter	Value
Robot mass	11.00 kg
Leg uncompressed length	0.25 - 0.38 m
Spring stiffness	1000 - 6000 N/m
Hip joint distance	0.54 m
Body inertia	2.917 $kg \cdot m^2$

The chassis is made of aluminum and is modular (Fig. 14), i.e. the body's length and width, and weight distribution and symmetry are adjustable. This is accomplished by positioning the frame elements at different positions using a number of pre-drilled holes.

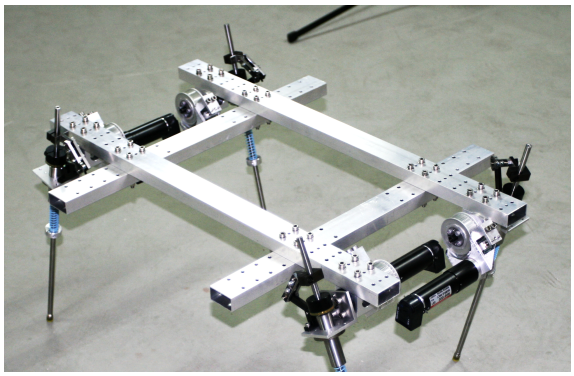

Figure 14. Body frame.

Legs are made of steel, for durability against impact forces, and consist of two main parts, i.e. upper and lower, and a spring coil to form a compliant prismatic joint, presented in Fig 15 (a). The lower part slides into the upper. The spring coil stores and transforms energy between the different phases of a gait. The design of the leg allows adjustments in the leg uncompressed length and the spring pre-tension. The leg's uncompressed length can be adjusted to a maximum of about 25% of the average leg length. In addition, the spring can be replaced easily to adjust leg compliance. The toes are made of shock absorbing material, which also keeps friction between the ground and the leg toes high.

An electric motor actuates each hip joint and places each leg to the desired angle, using a pulley-belt mechanism. Four full quadrature encoders fitted on each motor are used for leg angle measurements. Another four encoders incorporated in a 2-link mechanism, which transforms linear displacement to rotational, are used to measure spring compression (Fig 15 (b)). A 6 degrees of freedom inertial measurement unit (IMU) is mounted on the robot's body at the CM. IMU measurements are used for monitoring, but also as feedback, i.e. pitch motion, to the controller. Table 4 displays information regarding the NTUA Quadruped.

Table 4. Robot's main components specifications.

Component	Description
Actuators	4 Maxon RE30 60W DC, 0.85 Nm
Amplifiers	4 AMC DZRALTE-012L080
Encoders	4 Avago HEDS-5540, 3Ch, 500 cpr (leg angle) 4 US Digital E4P, 2Ch, 360 cpr (spring compression)
IMU	1 Analog Devices ADIS 16354
Onboard PC	1 PC/104 256MB 650Hz
MCU	8 dsPIC 30F4012 (encoder reading) 2 ATMEL ATMEGA16 (IMU, dsPICs and PC/104 communication)
Power Supply	1 Siemens SITOP 24v 5A (electronics, PC/104), 1 Siemens SITOP 24v 25A (motors) or Li-Po battery packs
Oper. Syst.	Arch Linux, kernel 2.6, RTAI patch

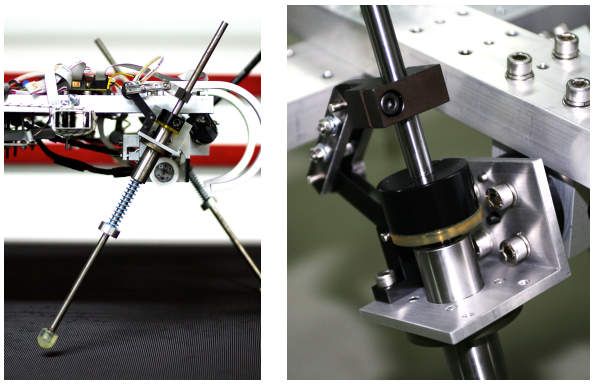

(a) (b)

Figure 15. (a) Leg. (b) Leg length measurement mechanism.

4.2. Experiments

The experiments conducted with the NTUA Quadruped robot and using the same multipart controlled that used in the simulations. In each experiment, the robot is released from an initial height of approximately 0.05m above the ground. This way of starting is necessary for achieving an initial spring compression, and thus energy accumulation. The robot continues its periodical motion through the separate phases that characterize each gait and described in Section 2. The basic goal of these experiments is to validate the simulation environment. Moreover, we examine how leg spring stiffness and length affects the overall motion and stability.

The multipart controller guides the quadruped robot to realize gaits with desired forward speed between 0.8 to 1.0 m/s and apex height around 0.29 – 0.32 m depending on leg uncompressed length. The body pitch angle rate is kept around 0 degs / s.

Fig. 16 and 17 present the body pitch angle and the forward speed data from the IMU sensor.

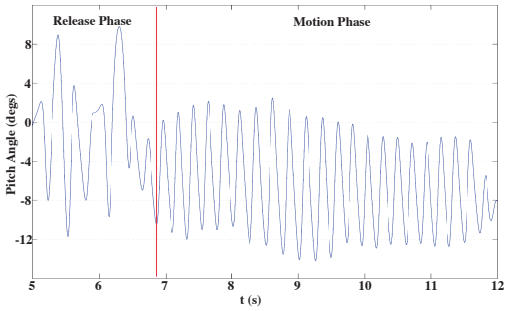

Figure 16. Body pitch angle. Data from the IMU sensor.

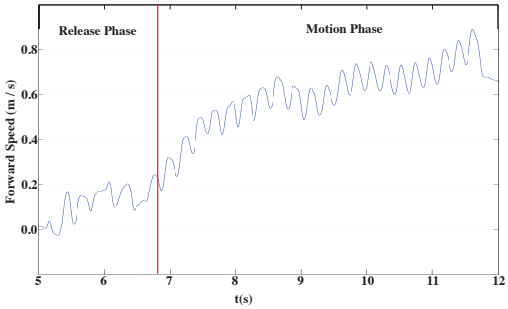

Figure 17. Forward Speed. Data from the IMU sensor.

5. CONCLUSIONS

This paper presented simulation results obtained with a quadruped robot on sloping ground. A multipart controller that exploits a novel transfer mechanism to achieve stable gaits with specific motion characteristics was employed. The front and rear VLegs are modeled in general to have different uncompressed length l_{0j}, spring constant k_j and viscous damping coefficient c_j. Simulations conducted to emulate a crater exploration mission scenario in Mars and Moon-like gravity environments.

Initial simulations were conducted to validate ideal values of VLegs spring constant when the quadruped robot traverses a level terrain in three different gravity environments that emulate Moon, Mars and Earth. The results show that a region for every environment can be identified that makes achievable different values of forward speed. Also, as gravity drops the leg springs need to be softer to accumulate energy. Moreover, the maximum achievable forward speed is lower in Mars and even lower in the Moon. In addition, as leg springs become stiffer, torque requirements increase. However, the use of softer springs leads to larger variations of robot body pitch angle.

During crater exploration, the quadruped achieved and maintained a dynamically stable motion with gaits of specific characteristics. In the case of a Mars-like gravity environment, the quadruped robot achieves and maintains a forward speed between 0.8 and 0.9 m/s during the mission, while the body pitch angle maximum values are ±4 degrees during transient phase. In the case of a Moon-like gravity environment, the quadruped robot achieves and maintains a forward speed between 0.4 and 0.5 m/s during the mission, while the body pitch angle maximum values are ±5.7 degrees during transient phase.

Experimental results with the physical prototype show that the NTUA Quadruped is capable of dynamically stable motion around desired motion characteristics. Further experiments will be conducted, using different leg springs and length values.

6. ACKNOWLEDGEMENTS

Part of this research has been co-financed by the European Union (European Social Fund –ESF) and Greek national funds through the Operational Program "Education and Lifelong Learning" of the National Strategic Reference Framework (NSRF) – Research Funding Program: Thalis. Investing in knowledge society through the European Social Fund.

7. REFERENCES

1. ESA Exobiology Team Study (1999). Exobiology in The Solar System and The Search for Life on Mars, ESA SP-1231, *ESA Publications Division*.
2. Heverly, M. and Matthews, J. (2008). A Wheel-on-limb rover for lunar operation. *Proc. i-SAIRAS* 2008, Hollywood, USA.
3. Görner, M., Chilian, A. and Hirschmüller, H. (2010). Towards an Autonomous Walking Robot for Planetary Surfaces. *Proc. i-SAIRAS 2010*, Sapporo, Japan.
4. Chacin, M. and Yoshida, K. (2008). A Microgravity Emulation Testbed for Asteroid Exploration Robots. In Proc. i-SAIRAS 2008, Hollywood, USA.
5. Bartsch, S. et al. (2010). SpaceClimber: Development of a Six-Legged Climbing Robot for Space Exploration. *Proc. ISR/ROBOTIK* 2010, Munich, Germany.
6. Latta, M., Remy, C. D., Hutter, M., Höpflinger, M. and Siegwart, R. (2011). Towards Walking on Mars. In Symposium of Advanced Space Technology in Robotics and Automation, Noordwijk, Netherlands.
7. Raibert, M. (1986). *Legged Robots That Balance*, MIT Press, Cambridge, MA, pp. 92-95.
8. Siciliano, B., Sciavicco, L., Villani, L., Oriolo, G. (2010). *Robotics. Modeling, Planning and Control*, Springer-Verlag, London, pp. 247-257.
9. Cherouvim, N., Papadopoulos, E. (2010). Novel Energy Tranfer Mechanism in a Running Quadruped Robot with One Actuator per Leg. *Advanced Robotics*, 24(7), 963-978.
10. Chatzakos, P., Papadopoulos, E. (2009). Bio-inspired Design of Electrically-Driven Bounding Quadrupeds via Parametric Analysis. *Mechanisms and Machine Theory*, 44(3), 559-579.